

# A Combined Theoretical and Experimental Approach to Determining Order Parameters of Solutes in Liquid Crystals from $^{13}\text{C}$ NMR Data

Caterina Benzi,<sup>†</sup> Maurizio Cossi,<sup>†</sup> Vincenzo Barone,<sup>†</sup> Riccardo Tarroni,<sup>\*,‡</sup> and Claudio Zannoni<sup>‡</sup>

*Dipartimento di Chimica, Università Federico II, Complesso Monte S. Angelo, via Cintia, I-80126 Napoli, Italy, and Dipartimento di Chimica Fisica ed Inorganica and INSTM, Università di Bologna, viale Risorgimento 4, I-40136 Bologna, Italy*

*Received: September 10, 2004; In Final Form: December 2, 2004*

The ordering properties of an anisotropic liquid crystal can be studied by recording  $^{13}\text{C}$  NMR spectra at different temperatures for a number of rigid solutes. The traditional difficulty in analyzing  $^{13}\text{C}$  data comes from the scarcity of experimental information about the carbon shielding tensors and from their limited transferability among different solutes. We show that these obstacles can be overcome by computing high-level *ab initio* shielding tensors, also including the solvent effects by the polarizable continuum model. The reliability of this combined approach is carefully verified, and the order parameters of several solutes are obtained by reanalyzing previously published spectra. The quality of the results is shown to be comparable to deuterium NMR without the need of isotopic substitution.

## 1. Introduction

Understanding and controlling the alignment of organic solute molecules in anisotropic liquid crystal solutions is of crucial importance in many technological applications ranging from dye-based displays<sup>1</sup> to nanoorganized materials.<sup>2</sup> In a different context, ordering of solutes in weakly anisotropic media has proved to be very useful for obtaining average dipolar couplings and consequently structural data for proteins and other biomolecules in solution.<sup>3,4</sup> From a fundamental point of view, the accurate measurement of the orientational order parameters<sup>5</sup> of molecules dissolved in orienting media is essential to improve our understanding, still incomplete, of the molecular mechanisms leading to alignment in liquid crystalline phases and ultimately of the relevant intermolecular interactions in such systems.<sup>6</sup> In particular, detailed high-quality ordering data are needed to assess the relative importance of steric, dispersive, and electrostatic interactions for the alignment of rigid and flexible solutes, a topic of very active debate.<sup>6–9</sup>

Typically the obtainment of second rank order parameters of a molecule in liquid crystal solution is based on the experimental determination of the average anisotropy of a tensor property whose molecule fixed components are supposed to be known. Several spectroscopic quantities can be used for this purpose, but magnetic resonance techniques are particularly well suited and reliable.<sup>10–12</sup> Many studies are based on the dipolar coupling anisotropy in  $^1\text{H}$  NMR experiments, whose interpretation is however complicated by the large number of spectral lines that have to be analyzed, a problem that has limited the applicability of this approach, even with the aid of multiple quantum methods, to small solutes.<sup>11,13</sup> A possible solution is to resort to  $^2\text{H}$  NMR, where the anisotropic quantity is the deuteron quadrupole tensor: in this case the analysis of spectra

is easier, though the peak assignment is far from trivial.<sup>12</sup> The main limitation, however, is due to the unavoidable deuteration of the solute molecules, which makes this method too lengthy and expensive for many applications, and this has indeed limited the number of available sets of experimental data.

Another magnetic center that can be used to obtain orientational order information, and that does not require any preliminary synthetic step, is  $^{13}\text{C}$ : natural abundance  $^{13}\text{C}$  NMR of organic molecules dissolved in liquid crystals (or in other orienting media) can in principle employ the anisotropic chemical shielding tensor,  $\sigma$ , of each carbon atom as a local probe.<sup>14</sup> A method has been proposed some years ago to compute the solute order parameters from a sufficient number of independent shielding tensor anisotropies: the method is briefly summarized in the following and is exhaustively described in refs 15–17. This approach avoids many of the limitations of other NMR-based determinations of ordering properties: it has been successfully applied to find the ordering matrix of fused aromatic rings (e.g., naphthalene, pyrene, anthracene, and derivatives)<sup>15,16</sup> and of conjugated systems like *p*-bis(*o*-methylstyryl)benzene<sup>17</sup> in the nematic phase of the aliphatic liquid crystalline mixture ZLI-1167. The main obstacle to the extension of the method is that the  $^{13}\text{C}$  chemical shielding tensors are known only for a few systems:<sup>18</sup> the experimental technique illustrated in ref 15 can provide both the  $\sigma$  anisotropy and the order parameters, but it needs a sensible “starting point”, i.e., a rather accurate estimate of the shielding tensor for at least two chemically different carbon atoms of the solute. In the applications cited above, the  $\sigma$  elements were taken from solid-state measurements of benzene and naphthalene shielding tensors. Moreover, it was assumed that the  $\sigma$  values detected for the different carbon atoms could to some extent be transferable to the other more complex systems studied, for which a direct experimental measure was not available. This assumption, which is likely to be less and less reliable as the solute molecules become chemically different from the simple

<sup>†</sup> Università Federico II.

<sup>‡</sup> Università di Bologna.

\* Corresponding author: e-mail tarroni@ms.fci.unibo.it; phone +39 051 6446754; fax +39 051 2093690.

“models”, can be avoided if the shielding tensors for the actual solutes are obtained by rigorous quantum mechanical calculations.

This is not a simple task from the computational point of view: first, computing magnetic parameters with chemical accuracy requires high-level *ab initio* methods (and this has limited the past applications to rather small molecules), and moreover the full anisotropic  $\sigma$  tensor must be calculated, including to some extent the environmental effects (i.e., solute–solvent interactions), possibly taking into account also the dielectric anisotropy of the liquid crystal. Such calculations are now feasible for a large number of chemical systems of realistic size, using methods rooted in the density functional theory (DFT)<sup>19</sup> with some recently developed hybrid density functionals.<sup>20</sup> Solute–solvent interactions, on the other hand, can be effectively included in the calculation by means of the polarizable continuum model (PCM),<sup>21</sup> recently implemented also for the calculation of nuclear magnetic shieldings<sup>22</sup> and extended to anisotropic solvents, like nematic liquid crystals,<sup>23</sup> for which a dielectric tensor has to be defined instead of a simple dielectric constant.

Our modified approach for the determination of the orientational order can then be summarized as follows: the anisotropy of the <sup>13</sup>C nuclear magnetic shifts is measured at different temperatures for the chosen organic molecules dissolved in the nematic phase of a liquid crystal. The  $\sigma$  tensor elements and their principal components are computed at the DFT/PCM level for all the solute atoms and used to extract from the experimental spectra the order parameters of the solute as described in refs 15–17.

To verify the reliability of fully *ab initio* shielding tensors, we have chosen to apply the combined method to a set of molecules whose experimental <sup>13</sup>C data were previously obtained<sup>15–17</sup> and for which independent order parameter measurements from <sup>2</sup>H NMR are also available, i.e., naphthalene, anthracene, anthraquinone, pyrene, and perylene<sup>24–26</sup> dissolved in ZLI-1167. This procedure also provides an indirect route to check the accuracy of the computed tensors that takes into account possible medium effects and that is preferable, in our opinion, to the direct comparisons of individual components to the solid-state experimental values.

## 2. Methods

**2.1. Theory.** All the calculations have been performed using the PBE1PBE hybrid density functional (based on the Perdew, Burke, and Ernzerhof<sup>27</sup> correlation and exchange functionals, modified as reported in ref 20): as in all hybrid functionals, the exchange part is corrected by a prefixed amount of Hartree–Fock (nonlocal) exchange.<sup>28</sup> In particular, PBE1PBE is known to provide nuclear magnetic shieldings in excellent agreement with the experiment for a large number of organic molecules.<sup>29,30</sup> The 6-311+G(2d,p) basis set,<sup>31</sup> including diffuse functions<sup>32</sup> on heavy atoms and polarization functions<sup>33</sup> on all the atoms, has been employed in all the calculations. The chemical shielding tensors have been computed with the GIAO (gauge-independent atomic orbitals) method.<sup>34</sup>

Solute–solvent interactions are included by means of the polarizable continuum model (PCM):<sup>21</sup> the solvent is represented as an infinite dielectric medium, and the solute is embedded in a “cavity” formed by spheres centered on solute atoms and smoothed by adding some additional spheres, as described in ref 35, so that the solute–solvent boundary is realistically modeled on the solute shape. The solvent reaction field is expressed in terms of a set of apparent charges spread on the

cavity walls, self-consistently adjusted with the solute electron density. The solvation charges are determined by solving the Poisson equations with the suitable boundary conditions on the cavity walls: in the most recent formulation,<sup>21b</sup> the charges only depend on the electrostatic potential generated by the solute on the cavity surface.

In some applications,<sup>36</sup> it has been found that results are improved by including in the calculation some of the first shell solvent molecules explicitly (so that they become part of the “solute”): however, this is important especially in protic solvents, which can form hydrogen bonds with the solute, and it is not expected to be relevant in the present case. The model has also been extended to anisotropic solvents,<sup>23</sup> like nematic liquid crystals, for which a dielectric tensor has to be defined instead of a simple dielectric constant: in this case the distribution of solvation charges, and hence the molecular free energy and the electronic properties in solution, depend on the orientation of the solute with respect to the principal axes of the dielectric tensor. Recently, the anisotropic version of PCM has been reformulated so that the solvation charges are computed in terms of the solute electrostatic potential,<sup>23c</sup> with the same formal expression used for isotropic solvents. In general, PCM is particularly suitable for this kind of calculation, because the most recent implementations are highly efficient and require computational times close to those for isolated molecules.

**2.2. <sup>13</sup>C NMR Spectra and Data Analysis.** To make the paper more readable, we briefly recall here the key points of the data analysis procedure used to extract order parameters from measured chemical shifts. We refer to the original papers<sup>15,16</sup> for a more complete discussion and for details of the experimental setup and procedure. Here we just recall that all the solute molecules (Aldrich) were dissolved in the nematic liquid crystal ZLI-1167 (Merk), a ternary eutectic mixture of aliphatic mesogens (4'-propyl-, 4'-pentyl-, and 4'-heptyl-4-cyanobicyclohexyls)<sup>37</sup> with a probe concentration of approximately 3% in weight. All the spectra were recorded, for each sample, in an unique experiment running from isotropic (355 K) to about room temperature (307 K) in a single cooling sequence. Besides minimizing experimental artifacts, such an approach made the use of internal standards like tetramethylsilane unnecessary since, as shown below, the observables of interest are the differences, for each chemically different carbon of the probe, of the chemical shifts in the isotropic and in the nematic solutions. Some sample spectra of the molecules considered here can be found in ref 15.

The orientationally averaged chemical shift for the *J*th solute nucleus (i.e., the component of  $\sigma_J$  parallel to the external magnetic field **B**) can be written as

$$\sigma_J^{\text{aniso}} = \sigma_J^{\text{iso}} + \left(\frac{2}{3}\right)^{1/2} \langle \sigma_J^{\text{LAB}} \rangle \quad (1)$$

where  $\sigma_J^{\text{iso}}$  is a scalar contribution, which is the only one remaining in the isotropic phase, and  $\langle \sigma_J^{\text{LAB}} \rangle$  is the (2, 0) second rank spherical tensor component in the laboratory reference frame, averaged over the orientational distribution. This quantity can be related to the molecular order parameters, provided the reference frame is suitably rotated. A first rotation from the laboratory to the director (*d*) coordinate system is described by a simple multiplicative factor (assuming uniaxial symmetry for the liquid crystal around the director):  $\langle \sigma_J^{\text{LAB}} \rangle = S_f \langle \sigma_J^{\text{DIR}} \rangle$ . Because of the negative diamagnetic susceptibility of ZLI-1167, the director aligns perpendicularly to the external magnetic field and  $S_f = \langle P_2(\mathbf{d} \cdot \mathbf{B}) \rangle = -0.5$ .

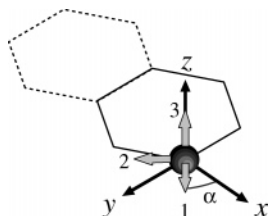


**Figure 1.** In-plane rotation  $\alpha$  relating the molecular ( $xyz$ ) frame to the principal (123) frame of an aromatic carbon tensor.

The orientation of the solute with respect to the director of the nematic phase is expressed in terms of second-rank order parameters  $\langle D_{0,n}^2 \rangle$ , averages of the Wigner rotation matrices transforming from the director to the molecular frame<sup>5</sup> once a suitable molecular axis system has been chosen. The molecules studied in this work all have  $D_{2h}$  symmetry, so that only two terms have to be considered:  $\langle D_{0,0}^2 \rangle \equiv \langle P_2 \rangle$ , i.e., the usual order parameter, the only one needed if the solute has effective uniaxial symmetry, and  $\langle D_{0,2}^2 \rangle$ , the molecular biaxiality order parameter:

$$\sigma_J^{\text{aniso}} - \sigma_J^{\text{iso}} = S_f \left[ \langle P_2 \rangle \sigma_{J:zz}^{\text{MOL}} + \left( \frac{2}{3} \right)^{1/2} \langle D_{0,2}^2 \rangle (\sigma_{J:xx}^{\text{MOL}} - \sigma_{J:yy}^{\text{MOL}}) \right] \quad (2)$$

where  $\sigma_{J:xx}^{\text{MOL}}$ ,  $\sigma_{J:yy}^{\text{MOL}}$ , and  $\sigma_{J:zz}^{\text{MOL}}$  are components of the Cartesian shift tensor in the molecular frame.

A final rotation, described by the Euler angles  $\alpha_J$ ,  $\beta_J$ , and  $\gamma_J$ , is needed to express the chemical shift in the principal (nuclear) frame, in which the shielding tensor for nucleus  $J$  is diagonal. The final expression for the shielding anisotropy of each chemically different  $^{13}\text{C}$  nucleus is then

$$\frac{\sigma_J^{\text{aniso}}(T) - \sigma_J^{\text{iso}}}{S_f} = [a_J \sigma_{J:33} + b_J (\sigma_{J:11} - \sigma_{J:22})] \langle P_2 \rangle(T) + [c_J \sigma_{J:33} + d_J (\sigma_{J:11} - \sigma_{J:22})] \langle D_{0,2}^2 \rangle(T) \quad (3)$$

where the temperature dependence of the measured shifts and of the order parameters have been explicitly indicated;  $\sigma_{J:11}$ ,  $\sigma_{J:22}$ , and  $\sigma_{J:33}$  are the components of the diagonal shift tensor (labeled from the least to the most shielded axes), and the geometrical factors  $a_J$ ,  $b_J$ ,  $c_J$ , and  $d_J$  are related to the Euler angles describing the orientation of the principal frame with respect to the chosen molecular frame:

$$a_J = \frac{3}{2} \cos^2 \beta_J - \frac{1}{2}$$

$$b_J = \frac{1}{2} \sin^2 \beta_J \cos 2\gamma_J$$

$$c_J = \left( \frac{3}{2} \right)^{1/2} \sin^2 \beta_J \cos 2\alpha_J$$

$$d_J = \left( \frac{1}{6} \right)^{1/2} [\cos 2\alpha_J \cos 2\gamma_J (1 + \cos^2 \beta_J) - 2 \sin 2\alpha_J \sin 2\gamma_J \cos \beta_J] \quad (4)$$

For the specific case of planar (or nearly) aromatic molecules, molecular and principal frames can be suitably chosen so that, for each carbon, they are simply related by a single  $\alpha_J$  rotation in the  $xy$  (molecular) plane, as shown in Figure 1.

**TABLE 1: Calculated in Vacuo Principal Components (ppm) of the  $^{13}\text{C}$  Shielding Tensors of Naphthalene Using the PBE1PBE Functional and Different Basis Sets<sup>a</sup>**

		C <sub>1</sub>	C <sub>2</sub>	C <sub>3</sub>
6-311+G(2d,p)	$\sigma_{11}$	109.6	101.7	73.7
	$\sigma_{22}$	11.0	6.9	71.5
	$\sigma_{33}$	-120.6	-108.6	-145.2
6-311+G(2d,2p)	$\sigma_{11}$	109.4	101.6	73.8
	$\sigma_{22}$	11.1	6.8	71.6
	$\sigma_{33}$	-120.6	-108.5	-145.4
6-311++G(2d,2p)	$\sigma_{11}$	109.6	101.7	74.5
	$\sigma_{22}$	11.0	6.6	71.0
	$\sigma_{33}$	-120.5	-108.3	-145.6

<sup>a</sup> Geometry calculated in vacuo at the PBE1PBE/6-31G(d) level. See Figure 2 for carbon labelings.

**TABLE 2: Calculated Principal Components (ppm) of Naphthalene  $^{13}\text{C}$  Shielding Tensors: Molecular Geometries Optimized with Different Basis Set and/or Environmental Conditions<sup>a</sup>**

		C <sub>1</sub>	C <sub>2</sub>	C <sub>3</sub>
6-31G(d) in vacuo	$\sigma_{11}$	109.6	101.7	73.7
	$\sigma_{22}$	11.0	6.9	71.5
	$\sigma_{33}$	-120.6	-108.6	-145.2
6-31+G(d,p) in vacuo	$\sigma_{11}$	109.4	101.6	73.6
	$\sigma_{22}$	11.0	6.8	71.5
	$\sigma_{33}$	-120.4	-108.4	-145.2
6-31G(d) in condensed phase	$\sigma_{11}$	109.5	101.8	73.4
	$\sigma_{22}$	11.0	6.7	71.6
	$\sigma_{33}$	-120.4	-108.5	-145.0

<sup>a</sup> NMR calculation using PBE1PBE/6-311+G(2d,p). See Figure 2 for carbon labelings.

### 3. Results

As pointed out in the Introduction, to validate the method and in particular the shielding tensor calculations, we have considered a set of condensed aromatic molecules whose order parameters in ZLI-1167, obtained from deuterium NMR spectra, are available. The set includes naphthalene, anthracene, anthraquinone, pyrene, and perylene. For these we can check the accuracy of our order parameters with those coming from  $^2\text{H}$  NMR, also comparing them to the parameters obtained from eq 3 when the carbon  $\sigma$  is taken from solid-state  $^{13}\text{C}$  NMR measurements (when available) or is assumed transferable from similar molecules.

First, we assessed the parameters of the ab initio calculation, using naphthalene as test system. In previous applications,<sup>30</sup> very satisfactory chemical shieldings were obtained for similar solutes at the PBE1PBE/6-311+G(2d,p)/PBE1PBE/6-31G(d) level. The naphthalene molecular geometry was then optimized in the gas phase at the PBE1PBE/6-31G(d) level, and the carbon shielding tensors were calculated in vacuo with different basis sets, with the results listed in Table 1: one can see that also in this case the above-mentioned approach is very close to the basis set convergence.

The solute geometry was then reoptimized with a larger basis set and adding solvent effects (using PCM to simulate an isotropic environment with dielectric constant  $\epsilon = 8.1$ , actually corresponding to the parallel component of the dielectric tensor; vide infra): the shielding tensors computed at the different geometries are compared in Table 2; even in this case, geometry rearrangement effects can be safely neglected, as could be expected for such quite rigid aromatic systems.

Finally, solvent polarization effects were evaluated by repeating the calculation in different environments. The dielectric tensor principal values for ZLI-1167 are  $\epsilon_{||} = 8.1$  (along the nematic director) and  $\epsilon_{\perp} = 4.0$  (perpendicular to the nematic

**TABLE 3: Solvent Effects on  $^{13}\text{C}$  Shielding Tensors (ppm) of Naphthalene<sup>a</sup>**

		C <sub>1</sub>	C <sub>2</sub>	C <sub>3</sub>
in vacuo	$\sigma_{11}$	109.6	101.7	73.7
	$\sigma_{22}$	11.0	6.9	71.5
	$\sigma_{33}$	-120.6	-108.6	-145.2
PCM: $\epsilon_{  }$ along X	$\sigma_{11}$	109.9	101.8	74.1
	$\sigma_{22}$	12.9	8.9	71.3
	$\sigma_{33}$	-122.7	-110.6	-145.3
PCM: $\epsilon_{  }$ along Y	$\sigma_{11}$	109.9	101.7	74.1
	$\sigma_{22}$	12.9	8.9	71.3
	$\sigma_{33}$	-122.8	-110.6	-145.3
PCM: $\epsilon_{  }$ along Z	$\sigma_{11}$	109.9	101.7	74.1
	$\sigma_{22}$	12.7	9.0	71.3
	$\sigma_{33}$	-122.6	-110.7	-145.4

<sup>a</sup> All NMR calculations are at the PBE1PBE/6-311+G(2d,p) level and PBE1PBE/6-31G(d) in vacuo geometry. Refer to Figure 2 for the molecular frame definition and carbon labelings.

director) at 1 kHz and  $T = 35\text{ }^\circ\text{C}$ .<sup>38</sup> In Table 3 we report the naphthalene carbon shieldings computed at the PBE1PBE/6-311+G(2d,p)/PBE1PBE/6-31G(d) level in the gas phase and in anisotropic PCM, with the solute molecule either perfectly

aligned or perpendicular to the nematic axis. It is apparent that the solvent affects the computed property significantly, so that its effects cannot be neglected in any quantitative study. On the other hand, the solvent anisotropy has a very limited influence in the present conditions; i.e., the shielding tensors are fairly independent of the solute orientation with respect to the nematic axis. (Incidentally, this allows the application of eq 3 in the form derived above, in which  $\sigma_J$  elements do not depend on the order parameters.) In conclusion, we decided to perform all the following calculations at the above-mentioned level, using PCM with the solute aligned with the nematic axis.

As one can see in Table 3, the carbon 3 shielding is less affected by the solvent. This is not surprising, given that carbon 3 is markedly less exposed to the solvent; actually, the PCM sphere built around it has only  $2.3\text{ \AA}^2$  not buried by other spheres, in contrast with carbons 1 and 2, whose exposed surfaces are  $20.3$  and  $20.8\text{ \AA}^2$ , respectively.

It is clear from eq 3 that if the components of the diagonal tensor, as well as the orientation of the local frame with respect to the molecular frame, are known for at least two carbon atoms, the molecular order parameters can be evaluated at any temperature from the corresponding measured chemical shift anisotropies. On the other hand, if more than two carbons are

**TABLE 4: Calculated and Experimental Principal Components (ppm) of the  $^{13}\text{C}$  Shielding Tensors<sup>a</sup>**

naphthalene	C <sub>1</sub>		C <sub>2</sub>		C <sub>3</sub>	
	calcd	expt <sup>b</sup>	calcd	expt <sup>b</sup>	calcd	expt <sup>b</sup>
$\sigma_{11}$	109.9	101.9	101.8	94.7	74.1	73.6
$\sigma_{22}$	12.9	13.1	8.9	13.4	71.3	67.3
$\sigma_{33}$	-122.7	-115.0	-110.6	-108.1	-145.3	-140.0
$\alpha$	36.6	36.0	80.0	79.0	0.0 <sup>f</sup>	80.0

anthracene	C <sub>1</sub>		C <sub>2</sub>		C <sub>3</sub>		C <sub>4</sub>	
	calcd	expt <sup>c</sup>	calcd	expt <sup>c</sup>	calcd	expt <sup>c</sup>	calcd	expt <sup>c</sup>
$\sigma_{11}$	109.4	(101.9)	102.2	(94.7)	81.4	68.6	84.1	80.5
$\sigma_{22}$	11.6	(13.1)	6.5	(13.4)	61.0	64.6	11.8	15.7
$\sigma_{33}$	-121.0	(-115.0)	-108.5	(-108.1)	-142.4	-133.3	-95.9	-96.2
$\alpha$	39.7	(36.0)	77.5	(79.0)	57.0	(0.0)	90.0	(90.0)

anthraquinone	C <sub>1</sub>		C <sub>2</sub>		C <sub>3</sub>		C <sub>4</sub>	
	calcd	expt <sup>d</sup>	calcd	expt <sup>d</sup>	calcd	expt <sup>d</sup>	calcd	expt <sup>d</sup>
$\sigma_{11}$	111.7	(102.4)	103.0	(100.3)	85.0	128.1	81.8	96.4
$\sigma_{22}$	20.6	(17.4)	29.4	(29.3)	29.1	13.4	28.3	19.5
$\sigma_{33}$	-132.2	(-119.8)	-132.4	(-129.3)	-114.1	-142.1	-110.1	-115.9
$\alpha$	31.0	(30.0)	84.7	(87.0)	30.5	(0.0)	0.0	(0.0)

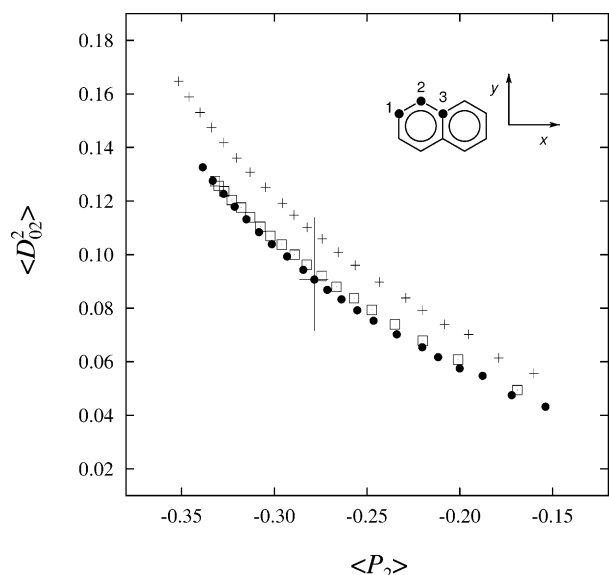
pyrene	C <sub>1</sub>		C <sub>2</sub>		C <sub>3</sub>		C <sub>4</sub>		C <sub>5</sub>	
	calcd	expt <sup>e</sup>	calcd	expt <sup>e</sup>	calcd	expt <sup>e</sup>	calcd	expt <sup>e</sup>	calcd	expt <sup>e</sup>
$\sigma_{11}$	110.7	102.7	96.4	87.4	99.7	95.7	82.5	82.0	74.2	73.7
$\sigma_{22}$	13.9	16.7	12.6	16.4	3.3	9.7	56.0	56.0	68.3	67.7
$\sigma_{33}$	-124.6	-119.3	-109.0	-103.6	-103.0	-105.3	-138.8	-138.0	-142.6	-141.3
$\alpha$	0.0	0.0	55.5	58.0	75.0	75.0	76.7	102.0	0.0	0.0

perylene	C <sub>1</sub>		C <sub>2</sub>		C <sub>3</sub>		C <sub>4</sub>		C <sub>5</sub>		C <sub>6</sub>	
	calcd	expt <sup>f</sup>	calcd	expt <sup>f</sup>	calcd	expt <sup>f</sup>	calcd	expt <sup>f</sup>	calcd	expt <sup>f</sup>	calcd	expt <sup>f</sup>
$\sigma_{11}$	110.1	103.2	99.3	94.7	71.9	69.2	66.7	66.7	88.4	88.5	98.8	92.4
$\sigma_{22}$	11.1	13.0	6.9	7.5	66.5	67.9	65.9	64.9	29.6	29.5	18.4	19.6
$\sigma_{33}$	-121.2	-116.2	-106.1	-102.2	-138.4	-137.1	-132.6	-131.5	-118.0	-118.0	-116.3	-112.1
$\alpha$	53.9	52.8	9.6	9.4	0.0	16.5	0.1 <sup>g</sup>	83.3	14.8	15.2	59.0	57.0

<sup>a</sup> The angle  $\alpha$  (degree) corresponds to a rotation in the  $xy$  plane relating the principal frame to the molecular frame. Other Euler angles  $\beta$  and  $\gamma$  are always set to zero. See Figures 2–6 for the definition of the molecular frames and the carbon labelings for the various molecules. <sup>b</sup> Solid-state values.<sup>40</sup> For equivalent carbons, average values have been taken. <sup>c</sup> From liquid crystal studies.<sup>16</sup> Values in parentheses are either taken from naphthalene<sup>40</sup> or assumed. <sup>d</sup> From liquid crystal studies.<sup>16</sup> Values in parentheses are either taken from acetophenone<sup>39</sup> or assumed. <sup>e</sup> Solid-state values.<sup>41</sup> For equivalent carbons, average values have been taken. <sup>f</sup> Solid-state values.<sup>42</sup> For equivalent carbons, average values have been taken. <sup>g</sup> The apparently large difference between calculated and experimental values is due to a switching between 1 and 2 principal value frame axes, which is in turn due to the similarity of  $\sigma_{11}$  and  $\sigma_{22}$  for bridge carbons.





**Figure 2.** Naphthalene in nematic ZLI-1167. Order parameter  $\langle D_{02}^2 \rangle$  plotted as a function of  $\langle P_2 \rangle$ , obtained either from  $^2\text{H}$  NMR<sup>24</sup> (empty squares) or  $^{13}\text{C}$  NMR, using solid state<sup>40</sup> (crosses) and ab initio (full circles)  $^{13}\text{C}$  shielding tensors. Order parameters error bounds estimated as described in the text.

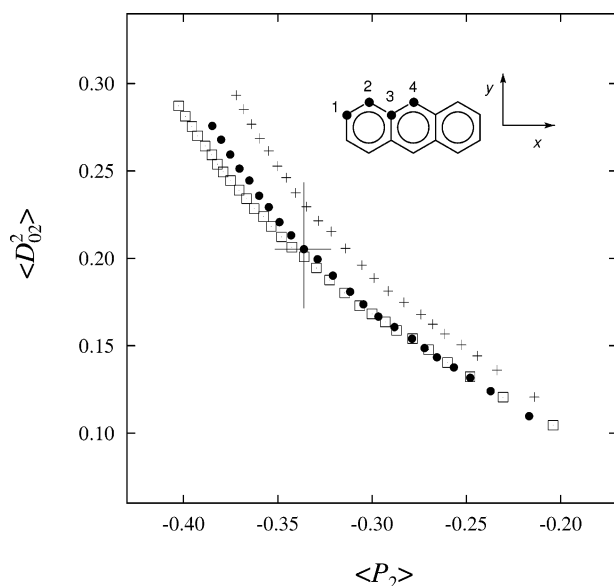


**Figure 3.** Anthracene in nematic ZLI-1167. Order parameter  $\langle D_{02}^2 \rangle$  plotted as a function of  $\langle P_2 \rangle$ , obtained either from  $^2\text{H}$  NMR<sup>25</sup> (empty squares) or  $^{13}\text{C}$  NMR, using naphthalene solid state<sup>40</sup> (crosses) and ab initio (full circles)  $^{13}\text{C}$  shielding tensors. Order parameters error bounds estimated as described in the text.

available, a least-squares fitting to order parameters is needed. In the procedure suggested here, both diagonal components and orientation of the local frame are computed theoretically at the level described above. These data are collected in Table 4 and compared to literature experimental solid-state values. The same values have been in turn used to recover order parameters from  $^{13}\text{C}$  NMR measurements.

In Figures 1–5 the biaxial order parameters  $\langle D_{0,2}^2 \rangle$  are plotted against  $\langle P_2 \rangle$  for the various solutes, each point corresponding to a different temperature in the nematic range. For naphthalene, pyrene, and perylene the single-crystal solid-state  $^{13}\text{C}$  NMR tensors are available, while for anthracene and anthraquinone we used tensor values borrowed from naphthalene and acetophenone, respectively. In the same figures we show the assumed molecular frame and the carbon labeling.

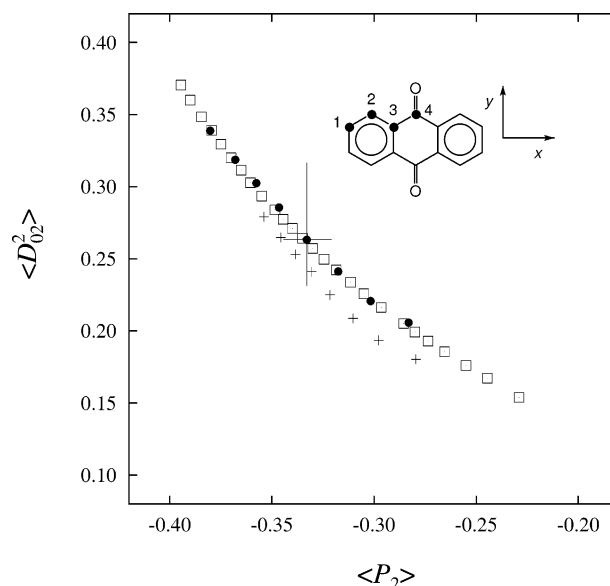


**Figure 4.** Anthraquinone in nematic ZLI-1167. Order parameter  $\langle D_{02}^2 \rangle$  plotted as a function of  $\langle P_2 \rangle$ , obtained either from  $^2\text{H}$  NMR<sup>25</sup> (empty squares) or  $^{13}\text{C}$  NMR, using acetophenone solid state<sup>39</sup> (crosses) and ab initio (full circles)  $^{13}\text{C}$  shielding tensors. Order parameters error bounds estimated as described in the text.

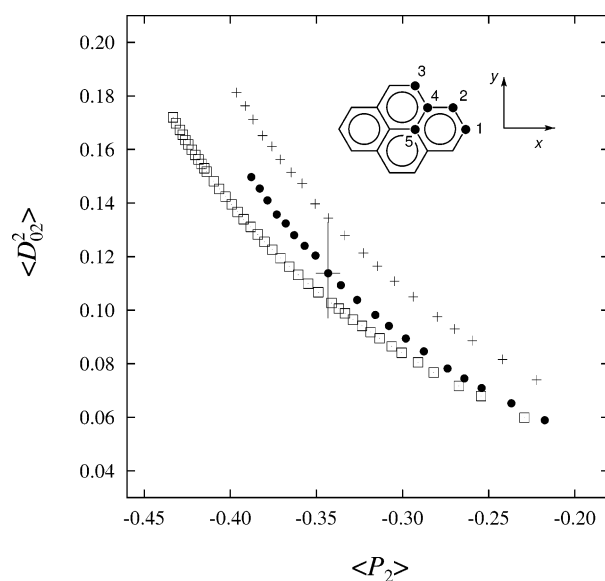


**Figure 5.** Pyrene in nematic ZLI-1167. Order parameter  $\langle D_{02}^2 \rangle$  plotted as a function of  $\langle P_2 \rangle$ , obtained either from  $^2\text{H}$  NMR<sup>26</sup> (empty squares) or  $^{13}\text{C}$  NMR, using solid state<sup>41</sup> (crosses) and ab initio (full circles)  $^{13}\text{C}$  shielding tensors. Order parameters error bounds estimated as described in the text.

It is evident that, for naphthalene, anthracene, and anthraquinone, the order parameters obtained using the theoretical values for the carbon  $\sigma$  are always in excellent agreement with those determined by deuterium NMR, while for pyrene and perylene the results are slightly less satisfactory. The results of the present procedure are markedly better than those obtained assuming the transferability of shielding tensors: this is not surprising, since the chemical environment of some, if not all, carbon atoms in fused aromatic systems is quite different from that in naphthalene or acetophenone. In addition, and more unexpectedly, for naphthalene and pyrene using the theoretical shieldings provides a better agreement with  $^2\text{H}$  NMR than using the single-crystal experimental shieldings. This result, in our opinion, cannot be attributed to the uncertainties of the

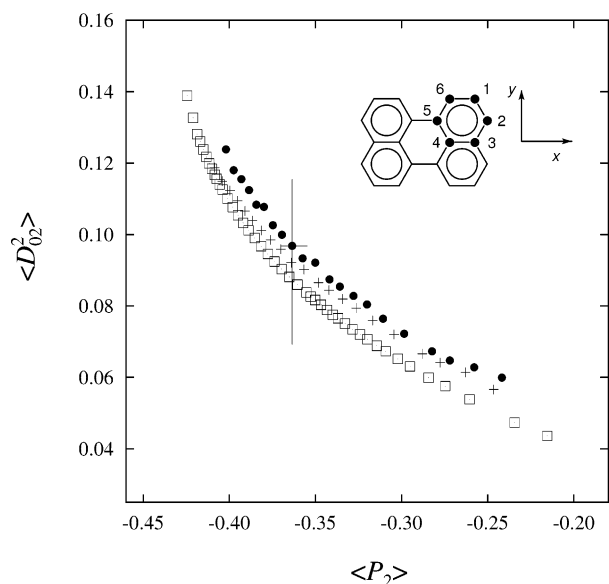


**Figure 6.** Perylene in nematic ZLI-1167. Order parameter  $\langle D_{02}^2 \rangle$  plotted as a function of  $\langle P_2 \rangle$ , obtained either from  $^2\text{H}$  NMR<sup>26</sup> (empty squares) or  $^{13}\text{C}$  NMR, using solid state<sup>42</sup> (crosses) and ab initio (full circles)  $^{13}\text{C}$  shielding tensors. Order parameters error bounds estimated as described in the text.

experimental values, since errors tend to compensate each other in the least-squares fitting to order parameters; instead, it points to some systematic drift induced by the crystal field to the carbon  $\sigma$  components. Computed shieldings, on the other hand, work better because systematic errors seem to be very small, and possible loss of accuracy in the individual tensor components or in the orientation tends to be smoothed by the data analysis procedure.

To better understand the effects of small errors, we have randomly varied the shielding tensors components and orientations of all chemically different carbons of each structure within a certain root-mean-square deviation (RMSD) from the calculated values. For this test we assumed a RMSD of 3 ppm for the principal value components and of  $2^\circ$  for the in-plane principal axis orientation. The procedure has been repeated several times ( $>10^3$ ), keeping a constant weight for all the experimental data points and monitoring the effects on the order parameters recovered by the analysis. The highest and the lowest values obtained both for  $\langle P_2 \rangle$  and for  $\langle D_{02}^2 \rangle$  give a reasonable guess of the errors on the order parameters, within the uncertainties assumed for the carbon shielding tensors. We found that these error bounds for  $\langle P_2 \rangle$  and  $\langle D_{02}^2 \rangle$  have a rather small temperature dependence; hence, to avoid an unnecessary crowding of Figures 2–6, we show only a sample value at a temperature in the middle of the nematic range.

The strict numerical agreement with the “deuterium” order parameters confirms that the PBE1PBE density functional is fully reliable for this kind of calculation and that short-range solvent effects are not relevant, so that there is no need to include some explicit solvent molecules in the calculation, as was expected for this kind of solute and for nonprotic solvents.

#### 4. Conclusions

We have developed a combined theoretical and experimental procedure to evaluate the order parameters of solutes in liquid crystals. The application of modern QM methods including solvent effects provides highly accurate carbon shielding tensors, which can be used in the analysis of experimental chemical shift anisotropies of organic solutes in nematics. This allows obtaining

order parameters of quality comparable to those obtained from deuterium NMR data. The method has been validated with a set of relatively simple aromatic molecules where independent experimental determinations of the orientational order were available. Analogous theoretical calculations can be performed even for significantly more complex molecules; when dealing with much larger systems, the calculations can anyway provide at least a set of chemical shift tensors for suitable molecular fragments which could be used to start the iterative procedure<sup>15</sup> previously used in connection with experimental data much more difficult or impossible to acquire. Compatibly with the intrinsic limitations of obtaining good quality  $^{13}\text{C}$  spectra in natural abundance samples, we believe that the method discussed here will prove a powerful addition to the tools employed to determine order parameters in a variety of applications.

**Acknowledgment.** We are grateful to MIUR (COFIN Cristalli Liquidi) and INSTM (PRISMA project) for support.

#### References and Notes

- (1) Bahadur, B., Ed. *Liquid Crystals, Applications and Uses*; World Scientific: Singapore, 1990.
- (2) Hamley, I. W. *Angew. Chem., Int. Ed.* **2003**, *42*, 1692.
- (3) Tjandra, N.; Bax, A. *Science* **1997**, *278*, 1111.
- (4) de Alba, E.; Tjandra, N. *Prog. Nucl. Magn. Reson. Spectrosc.* **2002**, *40*, 175.
- (5) Zannoni, C. In *Nuclear Magnetic Resonance of Liquid Crystals*; Emsley, J. W., Ed.; Reidel: Dordrecht, 1985; Vol. 141, p 1.
- (6) Burnell, E. E.; de Lange, C. A. *Chem. Rev.* **1998**, *98*, 2359.
- (7) Dingemans, T.; Photinos, D. J.; Samulski, E. T.; Terzis, A. F.; Wutz, C. *J. Chem. Phys.* **2003**, *118*, 7046.
- (8) Ferrarini, A.; Moro, G. J. *J. Chem. Phys.* **2001**, *114*, 596.
- (9) Celebre, G.; De Luca, G. *J. Phys. Chem. B* **2003**, *107*, 3243.
- (10) Dong, R. Y. *Nuclear Magnetic Resonance of Liquid Crystals*; Springer-Verlag: Berlin, 1997.
- (11) Burnell, E. E.; de Lange, C. A., Eds. *NMR of Ordered Liquids*; Kluwer Academic Publishers: Dordrecht, 2003.
- (12) Luckhurst, G. R.; Veracini, C. A., Eds. *The Molecular Dynamics of Liquid Crystals*; Kluwer: Dordrecht, 1994.
- (13) Celebre, G.; Castiglione, F.; Longeri, M.; Emsley, J. W. *J. Magn. Reson., Ser. A* **1996**, *121*, 139.
- (14) Fung, B. M. *Prog. Nucl. Magn. Reson. Spectrosc.* **2002**, *41*, 171.
- (15) Hagemeyer, A.; Tarroni, R.; Zannoni, C. *J. Chem. Soc., Faraday Trans.* **1994**, *90*, 3433.
- (16) Tarroni, R.; Zannoni, C. *J. Phys. Chem.* **1996**, *100*, 17157.
- (17) Tarroni, R.; Zannoni, C. *Chem. Phys.* **1996**, *211*, 337.
- (18) Duncan, T. *J. Phys. Chem. Ref. Data* **1987**, *16*, 125.
- (19) Parr, R. G.; Yang, W. *Density-Functional Theory of Atoms and Molecules*; Oxford University Press: New York, 1989.
- (20) Adamo, C.; Barone, V. *J. Chem. Phys.* **1999**, *110*, 6158.
- (21) (a) Miertus, S.; Scrocco, E.; Tomasi, J. *J. Chem. Phys.* **1981**, *55*, 117. (b) Cossi, M.; Scalmani, G.; Rega, N.; Barone, V. *J. Chem. Phys.* **2002**, *117*, 43.
- (22) Cammi, R.; Mennucci, B.; Tomasi, J. *J. Chem. Phys.* **1999**, *110*, 7627.
- (23) (a) Mennucci, B.; Cancès, E.; Tomasi, J. *J. Phys. Chem. B* **1997**, *101*, 10506. (b) Cancès, E.; Mennucci, B. *J. Math. Chem.* **1998**, *23*, 309. (c) Mennucci, B.; Cammi, R. *Int. J. Quantum Chem.* **2003**, *93*, 121.
- (24) Shilstone, G. N. Ph.D. Thesis, Southampton, 1986.
- (25) Emsley, J. W.; Hashim, R.; Luckhurst, G. R.; Shilstone, G. M. *Liq. Cryst.* **1986**, *1*, 437.
- (26) Shilstone, G. N.; Zannoni, C.; Veracini, C. A. *Liq. Cryst.* **1989**, *6*, 303.
- (27) Perdew, J. P.; Ernzerhof, M.; Burke, K. *J. Chem. Phys.* **1996**, *105*, 9982.
- (28) Becke, A. D. *J. Chem. Phys.* **1996**, *104*, 1040.
- (29) (a) Adamo, C.; Cossi, M.; Barone, V. *J. Mol. Struct. (THEOCHEM)* **1999**, *493*, 145. (b) Barone, V.; Crescenzi, O.; Improbato, R. *Quant. Struct. Act. Relat.* **2002**, *21*, 105.
- (30) Benzi, C.; Crescenzi, O.; Pavone, M.; Barone, V. *Magn. Reson. Chem.* **2004**, *42*, S57.
- (31) Frisch, M. J.; Pople, J. A.; Binkley, J. S. *J. Chem. Phys.* **1984**, *80*, 3265.
- (32) Petersson, G. A.; Al-Laham, M. A. *J. Chem. Phys.* **1991**, *94*, 6081.
- (33) Dunning, T. H., Jr. *J. Chem. Phys.* **1989**, *90*, 1007.
- (34) Wolinski, K.; Hilton, J. F.; Pulay, P. *J. Am. Chem. Soc.* **1990**, *112*, 8251.

- (35) (a) Pascual-Ahuir, J.-L.; Silla, E.; Tuñón, I. *J. Comput. Chem.* **1994**, *15*, 1127. (b) Cossi, M.; Mennucci, B.; Cammi, R. *J. Comput. Chem.* **1996**, *17*, 57. (c) Scalmani, G.; Rega, N.; Cossi, M.; Barone, V. *J. Comput. Methods Sci. Eng.* **2002**, *2*, 469.
- (36) Cossi, M.; Crescenzi, O. *J. Chem. Phys.* **2003**, *118*, 8863.
- (37) Wedel, H.; Haase, W. *Chem. Phys. Lett.* **1978**, *55*, 96.
- (38) Arcioni, A.; Bertinelli, F.; Tarroni, R.; Zannoni, C. *Mol. Phys.* **1987**, *61*, 1161.
- (39) Van Dongen Torman, J.; Veeman, W. S.; De Boer, E. *J. Magn. Reson.* **1978**, *32*, 49.
- (40) Sherwood, M. H.; Facelli, J. C.; Alderman, D. W.; Grant, D. M. *J. Am. Chem. Soc.* **1991**, *113*, 750.
- (41) Carter, C. M.; Alderman, D. W.; Facelli, J. C.; Grant, D. M. *J. Am. Chem. Soc.* **1987**, *109*, 2639.
- (42) Iuliucci, R. J.; Phung, C. G.; Facelli, J. C.; Grant, D. M. *J. Am. Chem. Soc.* **1996**, *118*, 4880.